ORGANOMETALLICS

ARTICLE

pubs.acs.org/Organometallics

Coordination Chemistry of a Hemilabile Amino-Tethered N-Heterocyclic Carbene with Ruthenium(II)

Howard Jong, Brian O. Patrick, and Michael D. Fryzuk*

Department of Chemistry, The University of British Columbia, 2036 Main Mall, Vancouver, BC, Canada V6T 1Z1

Supporting Information

ABSTRACT: The reaction of the amine-tethered N-heterocyclic carbene ligand 2,4,6-$Me_3C_6H_2NC_3H_2NCH_2CH_2NH$-2,4,6-$Me_3C_6H_2$ (^{Mes}[CNH]) with $Ru(CHPh)(PCy_3)_2Cl_2$ leads to the formation of ^{Mes}[CNH]$Ru(CHPh)(PCy_3)Cl_2$, which exists as a mixture of two isomers in a ratio of 7:1. While the major species was characterized by X-ray crystallography, the minor rotamer species could be characterized only in solution. Phosphine exchange kinetics and equilibrium variable-temperature measurements did not show much difference from benchmark Grubbs systems. Evidence for coordination of the amine tether was obtained by addition of pyridine, which generated the octahedral complex ^{Mes}[CNH]$Ru(CHPh)(py)Cl_2$ with the tethered amine coordinated. Similarly, addition of PMe_3 results in the formation of ^{Mes}[CNH]$Ru(CHPh)(PMe_3)Cl_2$, also having an octahedral structure with the pendant amine ligated. Attempts to benchmark the catalytic potential of the PCy_3 derivative showed that it was far inferior to known Grubbs-type systems.

INTRODUCTION

In the search for more efficient catalysts, ancillary ligand modifications on a proven catalyst precursor are a useful approach to try to augment catalyst activity. This is certainly evident in the evolution of ruthenium-based metathesis catalysts, for which improved versions have been discovered by substituting one of the phosphine ligands by various N-heterocyclic carbene (NHC) ligands.[1−4] The discovery that the lability and reassociative behavior of the ligand *trans* to the NHC are critical to the efficacy was made by a number of different groups, which allowed significant improvements in catalyst activity.[4−8] A number of other system changes have been made, for example, an examination of the effect of substituting the chlorides has been published.[9−11] One of the most intriguing changes was the discovery[12−15] that the use of a phosphonium-alkylidene precursor could dramatically improve the initiation step. However, for the most part, monodentate NHC systems have been the focus of these modifications.[1] In this study, we report our studies on the effects of having a potentially chelating NHC ligand coordinated to these ruthenium-based systems.

Our approach to ligand modifications relevant to this system was to examine the incorporation of a bulky hemilabile amino arm onto the NHC and monitor its effect in stabilization of unsaturated intermediates. We also were interested in the potential of a dangling amine to engage in secondary interactions with a substrate. While this ligand modification turns out to be mostly deleterious to catalysis, there are some intriguing effects on the coordination chemistry of these ruthenium benzylidene complexes that can be used to rationalize the observed modest catalytic efficiency.

RESULTS AND DISCUSSION

Synthesis and Characterization of ^{Mes}[CNH]$Ru(CHPh)(PCy_3)Cl_2$. Analogues of the Grubbs catalyst are relatively straightforward to synthesize, as substitution of the phosphine units of $Ru(CHPh)(PCy_3)_2Cl_2$ (**1**) occurs quite readily when strongly σ-donating Lewis bases are added. We have previously described the synthesis of the bidentate NHC ligand containing a mesitylamine tether, 2,4,6-$Me_3C_6H_2NC_3H_2NCH_2CH_2NH$-2,4,6-$Me_3C_6H_2$ (^{Mes}[CNH]).[16] The addition of a single equivalent of **2** to a Grubbs first-generation bis(phosphine) catalyst[17] in a solution of toluene at room temperature generates the expected ^{Mes}[CNH]$Ru(CHPh)(PCy_3)Cl_2$, **3**, product in good yield (eq 1).

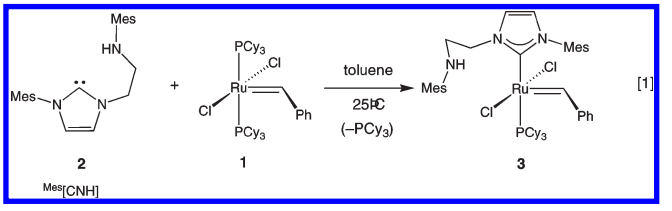

[1]

Complex **3** is fairly tolerant of air and moisture; however, it is best stored and handled under a dry inert atmosphere. It was characterized by the singlet in the ^{31}P NMR spectrum at δ 35.4 in addition to a diagnostic doublet at δ 187.8 in the ^{13}C NMR spectrum assigned to the NHC carbene carbon ($^2J_{CP}$ = 81 Hz). A small side product was detected in concentrated samples and is discussed below.

Received: January 28, 2011
Published: March 23, 2011

dx.doi.org/10.1021/om2000844 | *Organometallics* 2011, 30, 2333–2341

Table 1. Selected Bond Lengths and Angles for Compounds 3, 4, and 5[a]

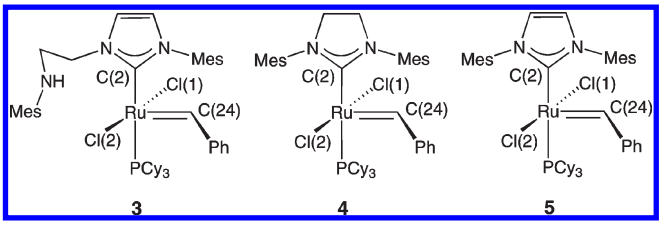

	3	4	5
	Bond Lengths (Å)		
Ru−C(2)	1.836(2)	1.835(2)	1.841(11)
Ru−C(24)	2.076(2)	2.069(11)	2.084(9)
Ru−Cl(1)	2.4138(6)	2.392(3)	2.382(3)
Ru−Cl(2)	2.3959(6)	2.383(3)	2.392(3)
Ru−P	2.4386(6)	2.419(3)	2.404(3)
	Bond Angles (deg)		
C(24)−Ru−C(2)	97.99(10)	99.2(5)	98.7(4)
C(24)−Ru−Cl(1)	89.88(8)	87.1(5)	90.0(3)
C(24)−Ru−Cl(2)	105.01(8)	104.3(5)	102.9(3)
C(2)−Ru−Cl(1)	87.09(6)	86.9(3)	83.0(3)
Cl(1)−Ru−P	90.04(2)	89.86(9)	89.86(9)
Cl(1)−Ru−Cl(2)	165.06(2)	168.62(12)	166.96(9)
C(24)−Ru−P	99.61(8)	97.1(4)	93.5(3)
C(2)−Ru−P	162.31(7)	163.2(3)	167.1(3)

[a] Atom labels have been renamed for simplicity in comparative analysis.

Magenta crystals of **3** suitable for single-crystal X-ray diffraction studies were obtained by slowly evaporating a concentrated solution of methylene chloride; the solid-state molecular structure is depicted in Figure 1. The slightly distorted square-pyramidal geometry of **3** is consistent with comparable analogues all having the benzylidene unit (C24) at the apical position. Table 1 outlines selected bond lengths and angles of **3** with its most similar structural counterparts, Grubbs second-generation catalyst **4**[4,18] and the IMes congener **5**.[3]

From inspection of the core bond lengths and angles of **3**, **4**, and **5**, it is clear that there are negligible structural differences between them (Table 1). For example, the Ru(01)−C(02) bond length of 2.076(2) Å for compound **3** is in between the values of 2.069(11) and 2.084(9) Å for **4** and **5**, respectively. The Ru(01)−C(24) benzylidene bond length of **3** was found to be virtually identical to that of **4**, at 1.836(2) Å. The Ru(01)−P(01) bond length of 2.4386(6) Å for **3** was found to be slightly longer than that of **4**, at 2.419(3) Å, and that of **5**, at 2.404(3) Å. Similarly, the bond angles for species **3**−**5** were comparable and varied only within a few degrees of each other. Typical of many of these kinds of complexes, the Ru=C−H plane is oriented so that there is quasi π-stacking of the N-Mes group of the NHC and the phenyl of the benzylidene moiety. One final feature deserves mention, and that is that the dangling N-mesityl group is oriented away from the open site *trans* to the benzylidene unit, thus precluding coordination.

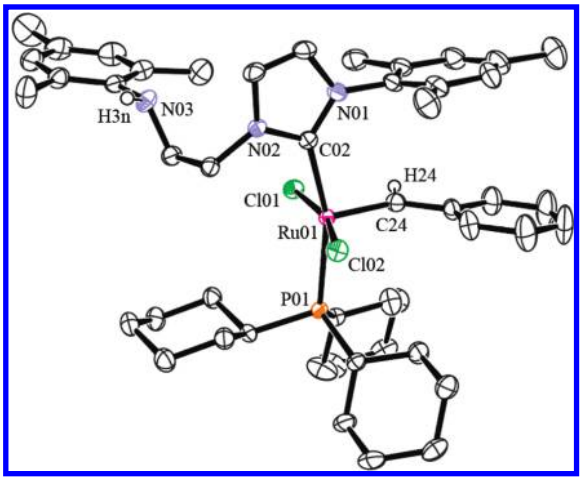

Figure 1. ORTEP view of ^{Mes}[CNH]Ru(CHPh)(PCy_3)Cl_2, **3**, with thermal ellipsoids at 50% probability. All hydrogens were removed for clarity except H3n and H24, which were located in a difference map and refined isotropically.

Detection of an Isomer of 3. When concentrated samples of **3** are probed by NMR spectroscopy, a second species can be detected in small quantities with chemical shifts that are similar to those of **3**. We denote this isomer as **3a**. While all efforts to try to isolate this minor species failed, it could be partially characterized in solution spectroscopically. **3a** is most easily identified by its benzylidene resonance (denoted as H(24a)) at δ 20.08 in the ^{1}H NMR spectrum in an approximately 1:7 ratio compared to the benzylidene signal of **3** at δ 19.19. Interestingly, the resonance assigned to H(24a) is a doublet ($^3J_{HP}$ = 12.9 Hz) as opposed to the singlet characteristic of **3**; it should be noted that the related ruthenium benzylidene complexes with SIMes, **4**, and IMes, **5**, all display singlets for the Ru=C(Ph)*H* moiety. This minor species can also be detected in the ^{31}P NMR spectrum of ^{Mes}[CNH]Ru(CHPh)(PCy_3)Cl_2, which displays two singlets at δ 35.4 and 22.8 for **3** and **3a**, respectively, in approximately the same 7:1 integral ratio. Performing a ^{1}H{^{31}P} NMR experiment on the sample shows the δ 20.08 doublet collapse into a singlet, which confirms that the benzylidene C−H is coupled to the Ru-bound PCy_3. Further evidence of the correlation was provided by the ^{1}H/^{31}P heteronuclear multiple-bond correlation (HMBC) experiment, which demonstrated the three-bond correlation between H(24a) and PCy_3. No correlation was observed for H(24) with PCy_3 on **3**, consistent with the H(24) singlet resonance in the ^{1}H NMR spectrum. Both phosphines showed correlation with cyclohexyl protons, which supports the presence of two Ru-PCy_3 species in solution. Figure 2 depicts the ^{1}H/^{31}P long-range correlation spectrum.

There are two possible structures for the minor isomer **3a**. One is ***syn*-3a**, in which the two chloro ligands are *cis* disposed and the PCy_3 unit is *cis* to both the NHC and the benzylidene. In ***syn*-3a** the phosphine (PCy_3) is oriented *syn* to H(24a), which rationalizes the doublet observed in the ^{1}H NMR spectrum, as the dihedral angle between H(24a) and PCy_3 is close to 0°. The lack of coupling between H(24) and PCy_3 in **3** is likely the result of PCy_3 being oriented orthogonal to the benzylidene C−H plane (as shown in the crystal structure), which generates a dihedral angle close to 90°. As already mentioned, it is generally assumed that the orientation of the benzylidene plane results

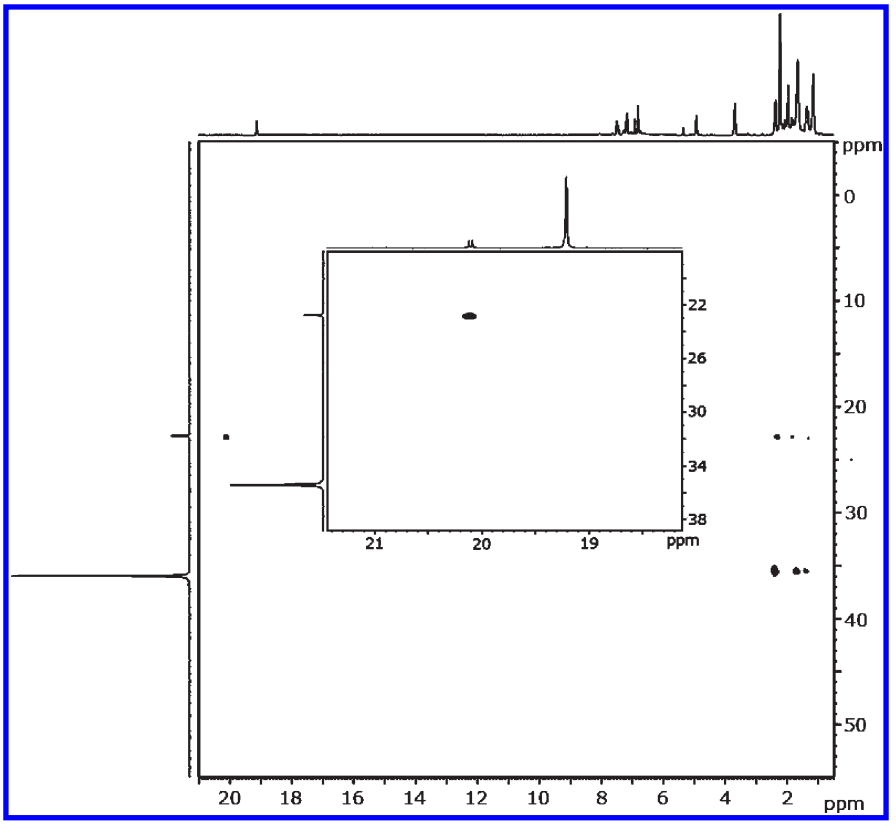

Figure 2. 400 MHz $^{1}H/^{31}P$ HMBC spectrum of **3** and **3a** in solution; inset focuses on the benzylidene−PCy_3 correlation.

from π-stacking of the N-Mes of the NHC and the benzylidene phenyl moiety.

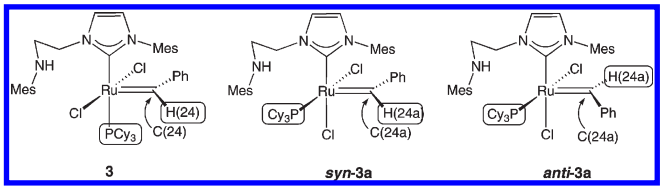

Another possible structure for the minor isomer **3a** is ***anti*-3a**, which can be considered as a geometric isomer of ***syn*-3a**, with the orientation of the PCy_3 unit and benzylidene C−H(24a) *trans* across the Ru═CHPh double bond. This stereoisomer has a dihedral of approximately 180°, which is consistent with the observed coupling of phosphorus-31 and this proton. However, ***anti*-3a** is more sterically crowded compared to ***syn*-3a**, as the former has the benzylidene phenyl oriented *cis* the bulky PCy_3 ligand.

There are other reports of modified ruthenium NHC benzylidene complexes for which the benyzlidene C−H appears as a doublet.[19,20] A minor isomer was also reported for the carbohydrate-modified NHC of **6**; in this case, the authors do not comment on the origin of the doublet but suggest that rotation about the Ru−NHC and Ru═CHPh bonds could lead to isomers.[19] More closely related to our dangling amine is the 2-hydroxyethyl-substituted NHC complex **7**, in which the authors confirm the isomeric form analogous to ***syn*-3a** by X-ray crystallography.[20] It is noteworthy that all of these systems that display a doublet for the benzylidene C−H proton incorporate unsymmetrical NHC units with one N-Mes substituent and an alkyl substituent with remote functionality, such as a carbohydrate (in **6**) or a hydroxyalkyl group (in **7**), or, in our case, the dangling aryl amine.

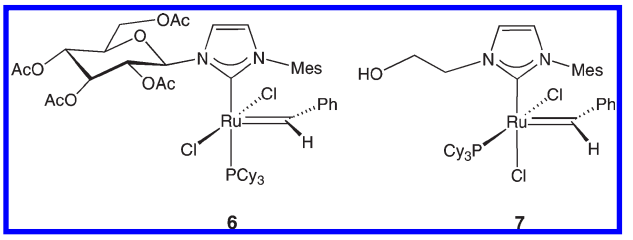

An inverse-gated ^{13}C NMR experiment on the mixture of **3** and **3a** was run on a 600 MHz spectrometer to provide quantitative integrations that further bolstered the presence of the two isomers in solution at room temperature. The doublet resonance at δ 306.0 ($J_{C(24)\text{-}P}$ = 12 Hz) was found in approximately a 1:7 ratio to the doublet at δ 294.5 ($J_{C(24)\text{-}P}$ = 7 Hz) representing complexes **3a** and **3**, respectively. A similar pattern was also found for the C(2)−P resonances at δ 187.8 ($J_{C(2)\text{-}P}$ = 81 Hz) and δ 182.7 ($J_{C(2)\text{-}P}$ = 104 Hz) for compounds **3** and **3a**, respectively, in a 7:1 ratio.

On the basis of variable-temperature ^{1}H and ^{31}P NMR experiments, these two isomeric forms were found to be in slow equilibrium; unfortunately, because of the rather small amounts of the minor isomer, we were unable to extract any thermodynamic information on the equilibrium or any kinetic data on

dx.doi.org/10.1021/om2000844 |*Organometallics* 2011, 30, 2333–2341

the rate of exchange. A similar observation was made for **6**, in which exchange between the major and minor isomers was detected by 2D NMR spectroscopy.

A rationale for the formation of minor isomer **3a** could likely be steric in nature, as there have been no reports of this type of isomerization occurring with similar systems containing large symmetrical NHC ligands such as SIMes or IMes with bulky phosphines like PCy_3 as in complexes **4** and **5**, respectively. The flexible and less sterically encumbering tether of the ^{Mes}[CNH] ligand in **3** would enable isomerization of the PCy_3 unit to a position that would presumably not be possible with two bulky NHC flanking substituents, such as N-mesityl groups. As mentioned above, analogous Ru complexes containing hydroxy-functionalized NHC ligands have previously been isolated that demonstrate the feasibility of this isomeric form in these systems.[20] Other similar Ru examples containing ligands that are less bulky are also known to exhibit *cis*/*trans* rearrangement.[21−23] Despite the presence of **3a**, the catalytic activity of **3** was explored, and the results demonstrate that the existence of this minor form **3a** in solution is largely inconsequential, particularly at higher temperatures.

RCM and ROMP Catalytic Reactions with ^{Mes}[CNH]Ru(CHPh)(PCy_3)Cl_2. Catalytic ring-closing metathesis (RCM) and ring-opening metathesis polymerization (ROMP) reactions of **3** were investigated and benchmarked with both **1** and **4**, Grubbs first- and second-generation catalysts, respectively, to determine the effects of incorporating the ^{Mes}[CNH] ligand. The olefin substrates selected for RCM were diethyl diallylmalonate (**S1**) and 1,6-heptadien-4-ol (**S2**). Diethyl diallylmalonate is commonly used as the benchmark[24] RCM substrate, whereas 1,6-heptadien-4-ol was chosen for its selectivity toward being effectively ring closed by Grubbs second-generation catalyst **4** while remaining inert to Grubbs first-generation catalyst, **1**.[4] The preferential reactivity of **S2** with an NHC-containing catalyst precursor allowed the effect of having a tethered NHC unit, as in **3**, to be explored. 1,5-Cyclooctadiene (**S3**) was selected for the ROMP study, as its results with various catalysts are well documented and easily employed as a benchmark[24] substrate.

Investigation of the RCM experiments using ^{Mes}[CNH]Ru(CHPh)(PCy_3)Cl_2 to catalyze **S1** and **S2** gave disappointing results. It was found that precursor **3** was completely inactive toward **S2** even at slightly elevated temperatures (40 °C), increased catalyst loadings (5 mol %), and long reaction times. Interestingly, the activity of **3** with **S1** also exhibited poor conversions and long reactivity times compared with Grubbs first (**1**) and second (**4**) generation catalysts. Selected results from the RCM test reactions are summarized in Table 2 with the corresponding reference catalysts.

Similar to that seen in Table 2, the modified ruthenium catalyst **3** with the dangling amine tether also underperforms as a ROMP catalyst when benchmarked to the standard catalysts, **1**, **4**, and **5**. Given that the bond lengths and bond angles listed in Table 1 do not indicate any significant structural differences between **3** and its analogues, it was necessary to investigate how else the presence of the ^{Mes}[CNH] ligand could negatively impact the RCM process and the metathesis mechanism. To probe the origin of the poor performance of **3**, details of the initiation step were studied.

Measurement of Phosphine Exchange Rates via Magnetization Transfer. It is commonly accepted that the active Ru metathesis catalyst is a 14-electron species generated via the dissociation of the tricyclohexylphosphine (PCy_3) ligand,[25−27] which directly correlates to the rate of catalyst initiation. Although the overall activity of the catalyst precursor does not correlate with this particular step, we wondered if the dangling amine arm could stabilize the 14-electron intermediate, which could be reflected by a difference in this rate compared to other systems.[18]

Table 2. RCM Results for 3 Compared with Reference Catalysts[24] under Similar Conditions

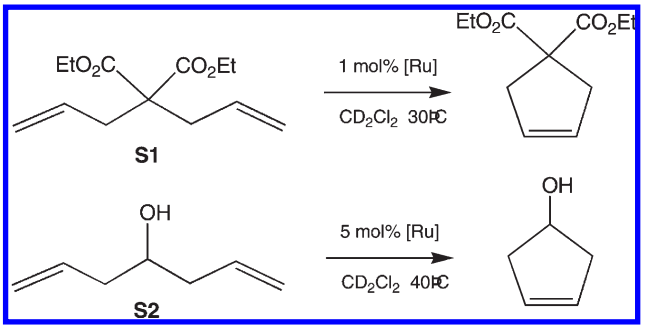

		conversion (%)[a]	
catalyst	time	S1	S2
1	30 min	66	
1	76 min	>74	
1[b]	24 h		no reaction
3	30 min	25	
3	18 h	50	
3	24 h		no reaction
4	30 min	96	
4	40 min	>98	
4[b]	10 min		>98
5	30 min	74	
5	80 min	>95	
5	N/A		

[a] Conversions measured by ^{1}H NMR spectroscopy. [b] Values obtained from the literature.[4]

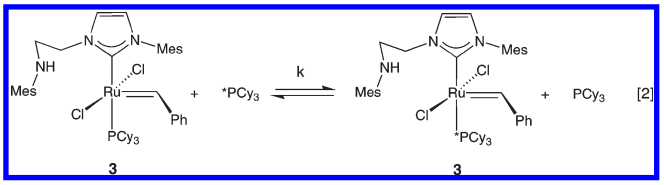

Magnetization transfer experiments using ^{31}P NMR spectroscopy were employed to probe the rate of phosphine exchange of **3** as shown in eq 2.[28] The time-dependent magnetization data were analyzed and fitted with CIFIT[29] software following that reported by others and the Eyring plot shown in Figure 3. The calculated rate constants and activation parameters for **3** are listed in Table 4 along with these same parameters for the reference catalyst precursors **1**, **4**, and **5**. As can be seen in the table, the activation free energies, $\Delta G^{\ddagger}$, for these different complexes are nearly identical especially for the NHC-based systems **3**, **4**, and **5**. Where the parameters differ for **3** is in the enthalpy and entropy of activation, which are considerably greater than those of other precursors. The calculated value for

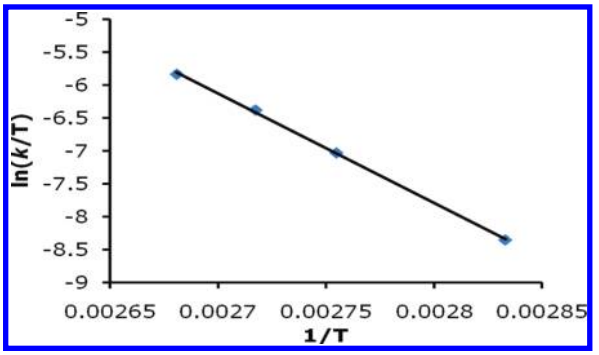

Figure 3. Eyring plot of phosphine exchange experiments for **3**.

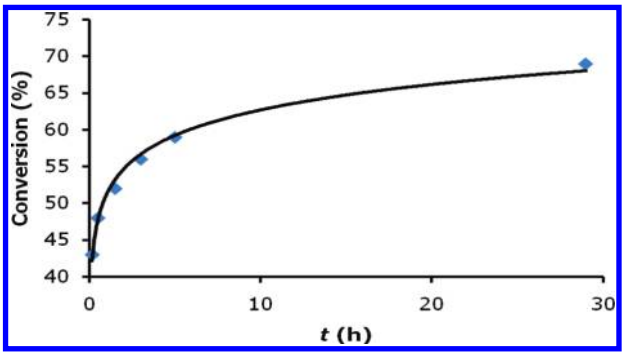

Figure 4. RCM conversion of **S1** at 100 °C in d_{10}-*o*-xylene using **3**.

$\Delta S^{\ddagger}$ of 30.2 ± 0.6 eu is certainly consistent with a dissociative process, but this value is much more positive than the values of 6−12 eu reported for **1**, **4**, and **5**. This could be attributed to the additional degrees of freedom due to the dangling amine arm of the ^{Mes}[CNH] ligand. What is clear is that the large positive value for $\Delta S^{\ddagger}$ is not consistent with association of the pendant amine during the exchange process.

While the kinetic data do not indicate any association of the amine tether in the phosphine exchange process, it could be that at lower temperatures a putative 18-electron complex, i.e., **3b**, would be favored, as shown by the equilibrium in eq 3. However, low-temperature NMR experiments were inconclusive, largely because of the presence of the minor isomer **3a**. Given the rather poor performance of **3** in RCM (see Figure 4 and Table 2) and ROMP attempts (see Table 3), we suggest that an equilibrium of this type could exist; however, it lies very much to the side of the 16-electron complex **3**. Given the large bulk of the N-mesityl group of the pendant amine and the fact that it would have to coordinate *cis* to the rather bulky PCy_3 unit, it is not surprising that we were unable to reliably detect **3b** in solution, even at low temperatures.

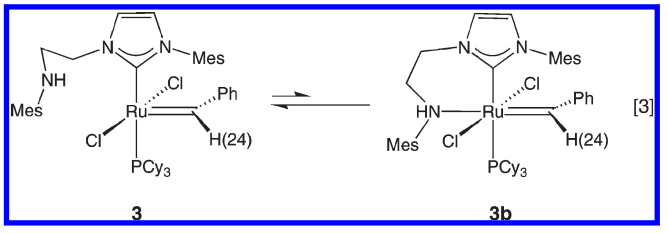

Synthesis and Characterization of ^{Mes}[CNH]Ru(CHPh)(py)Cl_2 and ^{Mes}[CNH]Ru(CHPh)(PMe_3)Cl_2. Comparative metathesis

Table 3. ROMP Results for 3 Compared[35] with Reference Catalysts under Similar Conditions

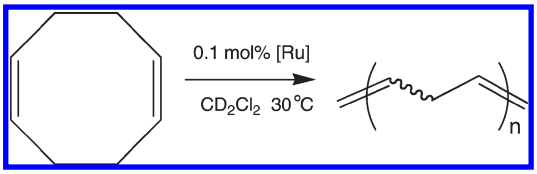

catalyst	time	conversion (%)[a]
1	90 min	~ 40
3	4 h	~ 75
4	6 min	>99
5	80 min	>99

[a] Conversions measured by ^{1}H NMR spectroscopy.

reactions with Ru precursors that contained different dissociating ligands could provide further insight into how the amino tether could interrupt the catalytic cycle. A common approach to synthesizing these analogues is to proceed through a mediating complex. The addition of pyridine to Ru precursors is known to displace the coordinated phosphine group to generate the bis(pyridine) species (IMes)Ru=CHPh(py)$_2$$Cl_2$ (**8**), which can be easily isolated and is reactive toward other phosphine ligands to yield Ru-PR_3 derivatives.[31]

When excess pyridine was added to complex **3**, as shown in Scheme 1, the result was not the anticipated bis(pyridine) species; rather it was the monopyridine product **9**, which has the pendant amine arm of the ^{Mes}[CNH] ligand coordinated to the Ru center. This 18-electron complex, ^{Mes}[CNH]Ru(CHPh)(py)Cl_2 (**9**), is, to the best of our knowledge, the first example of a Grubbs catalyst derivative incorporating a bidentate amino-NHC ligand. Compound **9** features a green color that is similar to the bis(pyridine)Ru complex **8**.[31] Single crystals suitable for X-ray diffraction studies for **9** can be grown via slow evaporation from a concentrated solution of toluene. The solid-state molecular structure is represented in Figure 5.

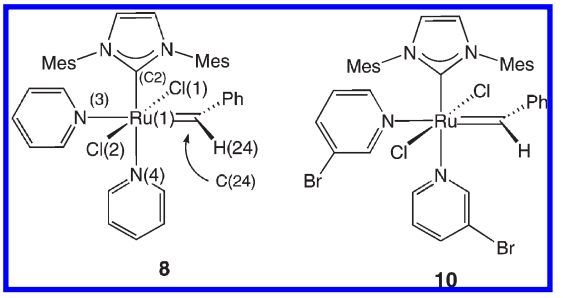

The geometry of ^{Mes}[CNH]Ru(CHPh)(py)Cl_2 is octahedral with bond lengths and angles that are consistent with analogous Ru complexes.[32,33] Comparisons of **9** can be made with **8** to highlight slight differences between them. The Ru(01)−N(04) distance of 2.173(2) Å in **9** was found to be marginally shorter than the 2.203(3) Å of **8**. However, the Ru(01)−N(03) distance of 2.516(5) Å in **9** (for the Ru-NHMesityl unit) is significantly longer than the comparable bond length of 2.372(2) Å in **8** (for the Ru-py ligand *trans* to the benzylidene). This is likely a result of both the bulk and the lower basicity of the pendant amine in **9** compared to the bound N(03)-positioned pyridine in **8**.[31]

dx.doi.org/10.1021/om2000844 |*Organometallics* 2011, 30, 2333–2341

Scheme 1

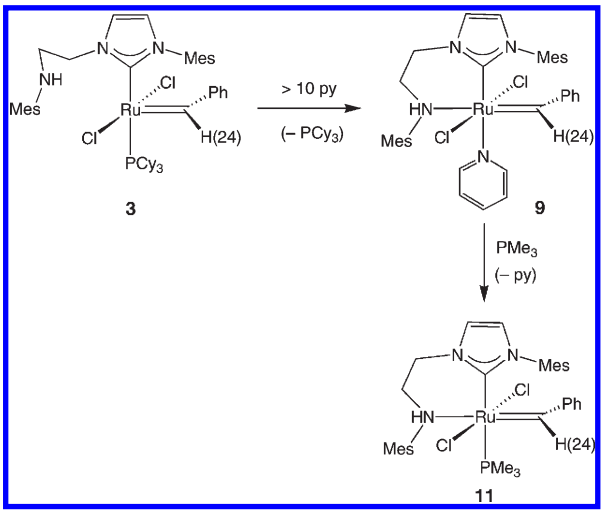

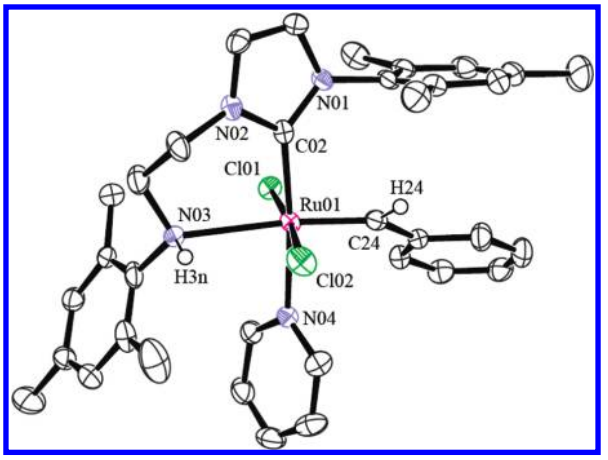

Figure 5. ORTEP view of ^{Mes}[CNH]Ru(CHPh)(py)Cl_2, **9**, with thermal ellipsoids at 50% probability. All hydrogens were removed for clarity except H3n and H24, which were located and refined isotropically.

Despite the presence of the potentially weakly coordinating amino tether of **9**, it was unreactive to addition of triphenylphosphine. However, addition of a smaller phosphine like trimethylphosphine to **9** yielded ^{Mes}[CNH]Ru(CHPh)(PMe_3)Cl_2 (**11**) as shown in Scheme 1. Complex **11** has a resonance at δ −14.3 and was absent of the free PMe_3 resonance at δ −62 in the ^{31}P NMR spectrum. The lack of resonances attributed to the pyridine unit and the observation of a PMe_3 doublet at δ 0.78 (J_{HP} = 8.8 Hz) in the ^{1}H NMR spectrum corroborated the ligand substitution. A solid-state molecular structure of **11** was obtained and is shown in Figure 6.

Structurally, **11** possesses similar characteristics to **9**. The two were differentiated most significantly by the C(02)−Ru(01) bond length of 2.0921(17) Å, which was more comparable to **3**. The Ru−N(03) bond length in **11** of 2.5786(15) Å was also found to be slightly longer than that in **9** at 2.516(5) Å. Having isolated a second example demonstrating the coordinative ability of the amino unit of the ^{Mes}[CNH] ligand, the assumption that the tethered arm of **3** is disruptive in the

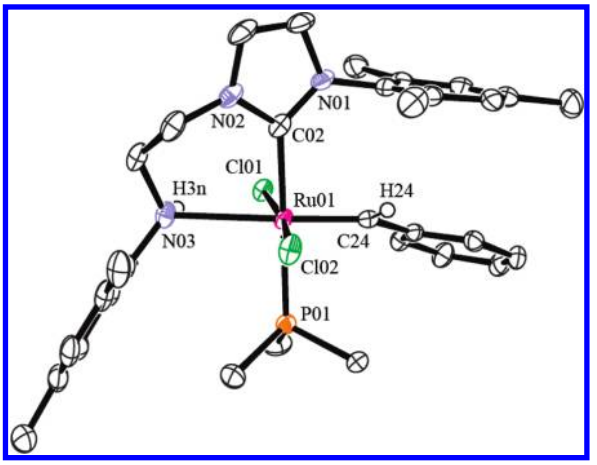

Figure 6. ORTEP view of ^{Mes}[CNH]Ru(CHPh)(PMe_3)Cl_2, **11**, with thermal ellipsoids at 50% probability. All hydrogens were removed for clarity except H3n and H24, which were located and refined isotropically.

catalytic cycle of olefin metathesis becomes more convincing. The propensity of coordination of the amino arm (as described by **3b** in eq 3) appears to be highly dependent on the steric bulk of its flanking ligand. The difference in size of pyridine and PMe_3 relative to PCy_3 is clearly the determining factor, as it enables the amino tether to coordinate to the ruthenium center. It is unclear at this point whether coordination of the dangling amine unit is favored given the orientation and bulk of the PCy_3 ligand. However, it is highly likely that coordination occurs once PCy_3 has dissociated from the metal center and could affect the alkene-binding step. As already mentioned, from the magnetization transfer experiments of **3**, it appeared that the propensity to bind the pendant amine did not significantly affect the rate of phosphine exchange, in the absence of added substrate.

Attempts to regenerate **3** via the addition of PCy_3 would be expected to fail, as the cone angle of PCy_3 (170°) is larger than that of PPh_3 (145°).[34] Yet **3** can indeed be regenerated by the addition of PCy_3 to complex **9**, but only to a maximum yield of 29% after 24 h, as indicated by ^{31}P NMR spectroscopy. The result implies that the electronic properties of the phosphine ligands take precedence over steric bulk in these substitution examples, as the increased electron-richness of PCy_3 was sufficient to displace the coordinated pyridine on **9** (albeit in low conversion) despite its larger physical size relative to PPh_3. The result differs greatly from those of **8**, which had demonstrated its coordinated pyridine ligands were substitutionally labile to PCy_3, PPh_3, and even electron-deficient phosphines such as P(*p*-$CF_3C_6H_4$)$_3$.

The bis(pyridine) complexes **8** and **10** are efficient metathesis precursors for both RCM and ROMP.[31,35] However, the monopyridine complex **9** is decidedly poor at catalyzing the conversion of the test substrates **S1** and **S2** (see Table 2) and **S3** (see Table 3). Using similar conditions[24] to that indicated for catalyst precursor **3**, it was observed that conversion RCM of **S1** reached only 10% after 12 h, RCM of **S2** reached 30% after 12 h, and ROMP of **S3** was measured to be 57% after 12 h (see Supporting Information). Such conversions are indicative of a catalyst that is even less efficient than **3**.

Even though we were unable to detect coordination of the tethered amine to the Ru center in the PCy_3 derivative **3**, the

Table 4. Rate Constants and Activation Parameters for Phosphine Exchange Experiments for 1, 3, 4, and 5

	k (s^{-1})					
catalyst	T = 40 °C[a]	T = 80 °C	T = 100 °C	$\Delta H^{\ddagger}$ (kcal/mol)	$\Delta S^{\ddagger}$ (eu)	$\Delta G^{\ddagger}$(25 °C) (kcal/mol)
3	$(2.00 \pm 0.07) \times 10^{-4}$	0.083 ± 0.004	1.09 ± 0.05	33.2 ± 0.6	30.2 ± 0.6	24.2 ± 0.6
4[b]	$(8.8 \pm 0.07) \times 10^{-4}$	0.13 ± 0.01	1.02 ± 0.02	27 ± 2	13 ± 6	23.0 ± 0.4
5[b]	$(2.8 \pm 0.07) \times 10^{-4}$	0.03 ± 0.01	0.23 ± 0.2	25 ± 4	6 ± 11	24 ± 1
1[b]	$(1.18 \pm 0.07) \times 10^{-4}$	9.6 ± 0.2[a]	63.0 ± 0.8	23.6 ± 0.5	12 ± 2	19.88 ± 0.06

[a] Values extrapolated from Eyring plots. [b] Data obtained from ref 30.

Table 5. Selected Bond Lengths and Angles for Complexes 8, 9, and 11, Respectively

	8[a]	**9**	**11**
Ru01−C02	2.033(4)	2.037(2)	2.092(2)
Ru01−N04	2.203(3)	2.173(2)	2.390(1)
Ru01−C24	1.873(4)	1.849(2)	1.860(2)
Ru01−N03	2.372(4)	2.516(5)	2.579(2)
Ru01−Cl01	2.400(1)	2.3849(7)	2.4136(4)
Ru01−Cl02	2.423(1)	2.4165(7)	2.4097(4)
C02−Ru01−C24	93.6(2)	94.1(1)	92.51(7)
C02−Ru01−N04	176.4(1)	173.51(8)	176.99(5)
C02−Ru01−N03	102.9(1)	88.7(1)	86.29(6)
C02−Ru01−Cl01	93.8(1)	92.45(7)	89.05(5)
C02−Ru01−Cl02	84.4(1)	87.36(7)	89.98(5)
C24−Ru01−N04	87.1(2)	91.62(9)	88.16(5)
C24−Ru01−N03	161.2(1)	170.8(2)	177.59(6)
C24−Ru01−Cl01	100.6(1)	97.54(8)	100.33(5)
C24−Ru01−Cl02	84.8(1)	88.08(8)	87.60(5)
Cl01−Ru01−Cl02	174.5(1)	174.37(2)	172.04(2)

[a] Bond lengths and angles taken from ref 31

isolation of **9** with the amine arm clearly coordinated is strong evidence that this substituent can coordinate when the metal center has sterically undemanding ligands like pyridine or PMe_3. Particularly noteworthy is the fact that when the pendant arm is coordinated as in the pyridine complex **9**, the catalyst efficiency is further reduced as compared to **3**.[36,37]

CONCLUSIONS

The original goal of this work was to examine the effect of the dangling amine tether of the modified NHC in ^{Mes}[CNH] on the catalytic efficiency of ruthenium-benzylidene precursor complexes in ring-closing metathesis and ring-opening metathesis polymerization processes. The square-pyramidal PCy_3 complex ^{Mes}[CNH]Ru(CHPh)(PCy_3)Cl_2, **3**, shows no evidence that the N-mesityl amine unit coordinates to the ruthenium center under equilibrium conditions to form putative **3b** (eq 3). Moreover, the activation energy of phosphine exchange for **3** is very similar to analogous NHC complexes that do not have dangling amine units, such as **4** or **5**. In addition, solid-state structural analyses of a series of NHC Ru benzylidene complexes show little variation in Ru−P, Ru−NHC, or Ru−C bond lengths, indicating that the ground-state structures of these complexes are very similar. It was therefore surprising to find that **3** underperformed in both RCM and ROMP when compared to the aforementioned benchmark catalyst precursors.

The addition of pyridine to **3** resulted in the formation of the monopyridine complex **9**, which also displayed very poor catalyst performance for RCM and ROMP. Given that this latter complex shows coordination of the N-mesityl amine group both in solution and in the solid state, it seems reasonable to suggest that the pendant amine is the source of the deleterious performance of the catalyst.

EXPERIMENTAL SECTION

General Considerations. Unless otherwise specified, all experimental procedures were performed in a dry, oxygen-free nitrogen or argon atmosphere by Schlenk or glovebox techniques. The NHC with the pendant N-mesityl amine, ^{Mes}[CNH], was synthesized as previously described.[16] 1,5-Cyclooctadiene was dried over activated 4 Å molecular sieves and distilled into a Teflon-sealed glass vessel. The Grubbs first generation catalyst Ru(CHPh)(PCy_3)Cl_2 (**1**) and all other chemicals were purchased commercially and used as received. Anhydrous toluene, hexanes, and pentane were purchased from Aldrich, sparged with nitrogen, and passed through columns containing activated alumina and Ridox catalyst. Methylene chloride and tetrahydrofuran were purified similarly, except without treatment with Ridox catalyst. Deuterated benzene (C_6D_6) was purified via refluxing under nitrogen with CaH_2, then vacuum transferred into a Teflon-sealed glass vessel containing 4 Å molecular sieves. Gases were removed by three freeze−pump−thaw cycles. Deuterated methylene chloride (CD_2Cl_2) was purified in a similar manner to C_6D_6. ^{1}H, ^{13}C, and ^{31}P NMR spectra were obtained by a Bruker AVANCE 300, 400, or 600 MHz spectrometer. Elemental analysis and mass spectrometry (EI/MS) were performed at the Department of Chemistry at the University of British Columbia.

^{Mes}[CNH]Ru(CHPh)(PCy_3)Cl_2 (3). A 5 mL toluene solution containing 507 mg (1.458 mmol) of ^{Mes}[CNH] was added slowly to 1.0 g (1.215 mmol) of Ru(CHPh)(PCy_3)$_2Cl_2$ dissolved in 10 mL of toluene. The resultant mixture was allowed to stir overnight. The solution was concentrated under vacuum, and hexanes was added to precipitate the magenta product, which was collected on a glass frit and washed with hexanes. Yield: 930 mg (86%). ^{1}H NMR (400 MHz, CD_2Cl_2) δ: 1.14 (br, −PCy_3), 1.36 (m, −PCy_3), 1.65 (br, −PCy_3), 1.95 (br, 6H, −ArCH_3), 2.22 (br, 9H, −ArCH_3), 2.40 − 2.32 (br, 6H, −ArCH_3, −PCy_3), 3.60 (br, 1H, −N*H*), 3.69 (m, 2H, −$N_{Mes}CH_2$), 4.94 (m, 2H, −$N_{imid}CH_2$), 6.80 (s, 2H, −Mes*H*), 6.88 (d, 1H, J = 1.7 Hz, −imid*H*), 7.32 − 7.07 (m, 6H, −Mes*H*, −Ar*H*), 7.43 (m, 1H, −Ar*H*), 7.47 (d, 1H, J = 1.7 Hz, −imid*H*), 19.19 (s, 1H, −RuC*H*Ph). ^{13}C NMR (151 MHz, CD_2Cl_2) δ: 18.50, 18.73, 20.86, 21.26, 21.70 (−ArCH$_3$), 27.23 (−PCy_3), 28.38 (d, J_{CP} = 9.7 Hz, −PCy_3), 30.06 (−PCy_3), 32.05 (d, J_{CP} = 16 Hz, −PCy_3), 48.96 (−$N_{Mes}CH_2$), 51.49, (−$N_{imid}CH_2$), 122.7, 124.1 (d, J_{CP} = 2 Hz, −imid*C*), 125.8, 129.5, 129.8 (−*m*-$Ar_{Mes}C$), 128.5, 128.7, 129.1 (−Ar*C*), 129.4, 131.1, 132.2, 136.6, 136.8, 139.1, 143.6 (−$Ar_{Mes}C_{ipso}$), 151.8 (−ArC_{ipso}), 187.8 (d, J_{CP} = 81 Hz, −RuC_{NCN}), 294.5 (d, J_{CP} = 7 Hz, −RuCHPh). ^{31}P{^{1}H} NMR (162 MHz, CD_2Cl_2) δ: 35.4 (s, Ru-*P*Cy_3). Anal. Calcd for

$C_{48}H_{68}N_3Cl_2PRu$: C, 64.78; H, 7.70; N, 4.72. Found: C, 65.04; H, 7.93; N, 4.89.

^{Mes}[CNH]Ru(CHPh)(py)Cl$_2$ (9). A 100 mg (0.1123 mmol) amount of ^{Mes}[CNH]Ru(CHPh)(PCy_3)Cl_2 was dissolved in 10 mL of toluene, and 1 mL of pyridine was added dropwise to the stirred solution. A color change from maroon to green is observed upon stirring for 10 min. The reaction was allowed to stir for 30 min total, at which time the solution was concentrated and pentane was added to afford a green suspension, which was cooled to −30 °C before filtration. The green product was dried under vacuum. X-ray suitable crystals can be grown via slow evaporation from a concentrated sample in methylene chloride. Yield: 50 mg (73%). ^{1}H NMR (400 MHz, CD_2Cl_2) δ: 2.04 (s, 3H, −ArCH_3), 2.06 (s, 3H, −ArCH_3), 2.28 (s, 6H, −ArCH_3), 2.42 (s, 6H, −ArCH_3), 3.61 (m, 2H, −N_{Mes}CH_2), 4.74 (m, 2H, −N_{imid}CH_2), 6.02 (t, 2H, J = 7.1 Hz, −*m*-pyH), 6.17 (s, 1H, −imidH), 6.42 (s, 1H, −imidH), 6.46 (br, 1H, −*p*-pyH), 6.51 (s, 2H, −MesH), 6.57 (s, 2H, −MesH), 6.95 (t, 2H, J = 7.1 Hz, −*m*-PhH), 7.23 (sh, 1H, −*p*-PhH), 7.30 (br, 1H, −NH), 8.16 (d, 2H, J = 7.1 Hz, −*o*-PhH), 8.50 (d, 2H, J = 6.1 Hz, −*o*-pyH), 19.8 (s, 1H, −RuCHPh). ^{13}C NMR (151 MHz, CD_2Cl_2) δ: 19.34, 20.81, 21.34, 21.53 (−$ArCH_3$), 51.19 (−$N_{Mes}CH_2$), 52.93 (−$N_{imid}CH_2$), 122.5 (−*m*-pyC), 123.2, 124.0 (−imidC), 127.8, 129.6, 129.7, 130.5, 131.5, 131.6 (−ArC), 132.5 (−ArC_{ipso}), 135.4 (−*p*-pyC), 137.5, 137.7, 138.6, 145.1, 153.3 (−ArC_{ipso}), 153.8 (−*o*-pyC), 185.1 (−RuC_{NCN}), 320.0 (−RuCHPh). Anal. Calcd for $C_{30}H_{40}N_4Cl_2Ru$: C, 61.04; H, 5.85; N, 8.14. Found: C, 61.21; H, 5.96; N, 8.47.

^{Mes}[CNH]Ru(CHPh)(PMe_3)Cl$_2$ (11). To a 10 mL toluene solution containing 110 mg (0.1597 mmol) of ^{Mes}[CNH]Ru(CHPh)(py)Cl_2 was added 0.02 mL (0.1940 mmol) of PMe_3 at room temperature. The green mixture was allowed to stir for 1 h and tested for completion periodically via unlocked ^{31}P{^{1}H} NMR. The solution was then concentrated, and hexanes was added to afford a dark green suspension. The suspension was chilled to −35 °C before being filtered. The green product was collected and washed with hexanes followed by drying under vacuum. X-ray suitable crystals can be grown via slow evaporation from a concentrated toluene solution. Yield: 74 mg (68%). ^{1}H NMR (400 MHz, C_6D_6) δ: 0.78 (d, 9H, J_{HP} = 8.8 Hz, −PCH_3), 1.91 (s, 3H, −ArCH_3), 2.15 (s, 9H, −ArCH_3), 2.6 (s, 6H, −ArCH_3), 3.39 (m, 2H, −N_{Mes}CH_2), 4.64 (m, 2H, −N_{imid}CH_2), 6.17 (s, 1H, −imidH), 6.21 (br, 1H, −NH), 6.35 (br, 3H, imidH, −MesH), 6.78 (s, 2H, −MesH), 7.02 (t, 2H, −*m*-PhH), 7.24 (t, 1H, −*p*-PhH), 8.29 (d, 2H, J = 7.5 Hz, −*o*-PhH), 20.0 (s, 1H, −RuCHPh). ^{13}C NMR (151 MHz, CD_2Cl_2) δ: 11.0 (d, J_{CP} = 25 Hz, −P(CH_3)$_3$), 16.1, 17.7, 18.1, 18.4 (−$ArCH_3$), 48.4 (−$N_{Mes}CH_2$), 50.03 (−$N_{imid}CH_2$), 122.9, 123.1 (d, J_{CP} = 3 Hz, imidC), 128.7, 128.8, 129.5, 129.6, 130.6 (−ArC), 131.7, 132.0, 132.1, 136.9, 137.9, 138.5,147.0, 154.3 (−ArC_{ipso}), 189.7 (d, J_{CP} = 100 Hz, −RuC_{NCN}), 311.0 (d, J_{CP} = 127, −RuCHPh). ^{31}P{^{1}H} NMR (162 MHz, C_6D_6) δ: −14.2 (s, −Ru-PMe_3). Anal. Calcd for $C_{33}H_{44}N_3Cl_2PRu$: C, 57.81; H, 6.47; N, 6.13. Found: C, 58.19; H, 6.78; N, 5.88.

Magnetization Transfer. A sealable J. Young NMR tube was charged with 17.0 mg (0.0191 mmol) of complex **3**, 8.0 mg (0.0287 mmol) of PCy_3, and 0.6 mL of d_{10}-*o*-xylene. The suspension was then allowed to thermally equilibrate at the experimental temperature, at which point the contents will have completely dissolved (minimum temperature of 80 °C required). The free PCy_3 resonance was selectively inverted via a 180° Gaussian 1.1000 shaped pulse with a duration of p22:50 ms at power level sp2. Twenty-one progressive mixing times ranging from 0.000003 to 30 s were run, and a subsequent nonselective 90° pulse was applied to record the FID. ^{1}H decoupling with WALTZ-16 was applied during the 90° pulse. Signal integrals of both the coordinated and free PCy_3 were analyzed with the CIFIT software to obtain phosphine exchange rate constants. Standard T_1 recovery experiments were performed at each temperature and analyzed with the CIFIT program. The pulse sequence and the values collected for the construction of the Eyring plot of **3** can be found in the Supporting Information. Eyring plot data for compounds **4**, **5**, and **1** were obtained from their original source.[30]

General Procedures for RCM of S1. To a Teflon-sealed J. Young NMR tube were added 1.650 μmol of Ru catalyst, 0.040 mL (0.1650 mmol) of diethyl diallylmalonate, and 0.60 mL of CD_2Cl_2. The sample was then heated to 30 °C, and conversion was determined by ^{1}H NMR using the ratio of methylene signals of the product relative to the substrate. Conversions of highly active catalysts are measured by equilibrating the sample containing the dissolved catalyst to 30 °C in the NMR probe before injection of the substrate via syringe.

General Procedures for RCM of S2. Procedures are as described for RCM of **S1** using 0.021 mL (0.1650 mmol) of 1,6-heptadien-4-ol, 8.250 μmol of Ru catalyst, and 0.62 mL of CD_2Cl_2.

General Procedures for ROMP of S3. Procedures are as described for RCM of **S1** using 0.020 mL (0.1650 mmol) of 1,5-cyclooctadiene, 0.10 mL of a 1.65 mM solution (0.1650 μmol) of Ru catalyst in CD_2Cl_2, and 0.52 mL of CD_2Cl_2.

X-ray Crystallographic Analysis. All crystals were mounted on a glass fiber and measured on a Bruker X8 diffractometer with graphite-monochromated Mo Kα radiation. The data were collected at a temperature of −100.0 ± 0.1 °C with the Bruker APEX II CCD area detector set at a distance of 36.00 mm. Data were collected and integrated using the Bruker SAINT[38] software package and corrected for absorption effects using the multiscan technique (SADABS).[39] The data were corrected for Lorentz and polarization effects, and the structure was solved by direct methods.[40] All non-hydrogen atoms were refined anisotropically, while all hydrogen atoms except those coordinated to the amino tether were placed in calculated positions but were not refined. Amino protons were located in a difference map and refined isotropically. All refinements were performed using the SHELXTL[41] crystallographic software package of Bruker-AXS. Selected bond lengths and angles of significant importance for **3**, **9**, and **11** are listed in Tables 1 and 5, respectively. For compound **9**, atoms N03 and H3n were found to be disordered and were modeled with their occupancies shared between two positions (N03/N03(b) and H3n/H3n(b)) in a ratio of 2:1.

■ ASSOCIATED CONTENT

Supporting Information. Details of the magnetization transfer experiments for **3** (pulse sequence, stacked plot, plot of normalized integrals, and the tabulated rate constants and T_1 values); table of RCM and ROMP results using **9** as a catalyst precursor; crystallographic data for **3**, **9**, and **11** (CIF). This material is available free of charge via the Internet at http://pubs.acs.org.

■ ACKNOWLEDGMENT

Funding for this research was provided by NSERC of Canada in the form of a Discovery Grant to M.D.F.

■ REFERENCES

(1) Samojlowicz, C.; Bieniek, M.; Grela, K. *Chem. Rev.* **2009**, *109*, 3708.

(2) Acherrmann, L.; Fürstner, A.; Weskamp, T.; Kohl, F. J.; Herrmann, W. A. *Tetrahedron Lett.* **1999**, *40*, 4787.

(3) Huang, J.; Stevens, E. D.; Nolan, S. P.; Petersen, J. L. *J. Am. Chem. Soc.* **1999**, *121*, 2674.

(4) Scholl, M.; Ding, S.; Lee, C. W.; Grubbs, R. H. *Org. Lett.* **1999**, *1*, 953.

(5) Garber, S. B.; Kingsbury, J. S.; Gray, B. L.; Hoveyda, A. H. *J. Am. Chem. Soc.* **2000**, *122*, 8168.

(6) Grela, K.; Harutyunyan, S.; Michrowska, A. *Angew. Chem., Int. Ed.* **2002**, *41*, 4038.
(7) Gessler, S.; Randl, S.; Blechert, S. *Tetrahedron Lett.* **2000**, *41*, 9973.
(8) Wakamatsu, H.; Blechert, S. *Angew. Chem., Int. Ed.* **2002**, *41*, 2403.
(9) Conrad, J. C.; Amoroso, D.; Czechura, P.; Yap, G. P. A.; Fogg, D. E. *Organometallics* **2003**, *22*, 3634.
(10) Conrad, J. C.; Parnas, H. H.; Snelgrove, J. L.; Fogg, D. E. *J. Am. Chem. Soc.* **2005**, *127*, 11882.
(11) Teo, P.; Grubbs, R. H. *Organometallics* **2010**, *29*, 6045.
(12) Romero, P. E.; Piers, W. E. *J. Am. Chem. Soc.* **2005**, *127*, 5032.
(13) van der Eide, E. F.; Romero, P. E.; Piers, W. E. *J. Am. Chem. Soc.* **2008**, *130*, 4485.
(14) Leitao, E. M.; van der Eide, E. F.; Romero, P. E.; Piers, W. E.; McDonald, R. *J. Am. Chem. Soc.* **2010**, *132*, 2784.
(15) van der Eide, E. F.; Piers, W. E. *Nat. Chem.* **2010**, *2*, 571.
(16) Jong, H.; Fryzuk, M. D. *Can. J. Chem.* **2008**, *86*, 803.
(17) Schwab, P.; Grubbs, R. H.; Ziller, J. W. *J. Am. Chem. Soc.* **1996**, *118*, 100.
(18) Love, J. A.; Sanford, M. S.; Day, M. W.; Grubbs, R. H. *J. Am. Chem. Soc.* **2003**, *125*, 10103.
(19) Keitz, B. K.; Grubbs, R. H. *Organometallics* **2010**, *29*, 403.
(20) Prühs, S.; Lehmann, C. W.; Fürstner, A. *Organometallics* **2004**, *23*, 280.
(21) Barbasiewicz, M.; Szadkowska, A.; Bujok, R.; Grela, K. *Organometallics* **2006**, *25*, 3599.
(22) Benitez, D.; Goddard, W. A. I. *J. Am. Chem. Soc.* **2005**, *127*, 12218.
(23) Diesendruck, C. E.; Tzur, E.; Ben-Asuly, A.; Goldberg, I.; Straub, B. F.; Lemcoff, N. G. *Inorg. Chem.* **2009**, *48*, 10819.
(24) Ritter, T.; Hejl, A.; Wenzel, A. G.; Funk, T. W.; Grubbs, R. H. *Organometallics* **2006**, *25*, 5740.
(25) Dias, E. L.; Nguyen, S. T.; Grubbs, R. H. *J. Am. Chem. Soc.* **1997**, *119*, 3887.
(26) Ulman, M.; Grubbs, R. H. *Organometallics* **1998**, *17*, 2484.
(27) Vyboishchikov, S. F.; Buhl, M.; Thiel, W. *Chem.—Eur. J.* **2002**, *8*, 3962.
(28) Sanford, M. S.; Ulman, M.; Grubbs, R. H. *J. Am. Chem. Soc.* **2001**, *123*, 749.
(29) Bain, A. D.; Kramer, J. A. *J. Magn. Reson.* **1996**, *118A*, 21.
(30) Sanford, M. S.; Love, J. A.; Grubbs, R. H. *J. Am. Chem. Soc.* **2001**, *123*, 6543.
(31) Sanford, M. S.; Love, J. A.; Grubbs, R. H. *Organometallics* **2001**, *20*, 5314.
(32) Abhur-Rashid, K.; Guo, R.; Lough, A. J.; Morris, R. H.; Song, D. *Adv Synth Catal* **2005**, *347*, 571.
(33) Occhipinti, G.; Bjorsvik, H. R.; Tornroos, K. W.; Jensen, V. R. *Organometallics* **2007**, *26*, 5803.
(34) Tolman, C. A. *Chem. Rev.* **1977**, *77*, 313.
(35) Love, J. A.; Morgan, J. P.; Trnka, T. M.; Grubbs, R. H. *Angew. Chem., Int. Ed.* **2002**, *41*, 4035.
(36) Anderson, D. R.; O'Leary, D. J.; Grubbs, R. H. *Chem.—Eur. J.* **2008**, *14*, 7536.
(37) Stewart, I. C.; Benitez, D.; O'Leary, D. J.; Tkatchouk, E.; Day, M. W.; Goddard, W. A., III; Grubbs, R. H. *J. Am. Chem. Soc.* **2009**, *131*, 1931.
(38) *SAINT*, Version 7.03A; Bruker AXS Inc.: Madison, WI, 1997−2003.
(39) *SADABS*, V 2.10; Bruker AXS Inc.: Madison, WI, 2003.
(40) Altomare, A.; Burla, M. C.; Camalli, M.; Cascaano, G. L.; Giacovazzo, C.; Guagliardi, A.; Moliterni, A. G. G.; Polidori, G.; Spagna, R. *J. Appl. Crystallogr.* **1999**, *32*, 115.
(41) *SHELXTL*, Version 5.1; Bruker AXS Inc.: Madison, WI, 1997.